



A semi-analytical solution for groundwater flow-field delineation near pumping/injection wells in confined aquifers

Ioan Bica¹ · Mohamed Amine Boukhemacha² · Ghiocel Groza³

Received: 15 February 2018 / Accepted: 30 August 2018 / Published online: 18 September 2018
© Springer-Verlag GmbH Germany, part of Springer Nature 2018

Abstract

A new semi-analytical solution to study groundwater flow fields associated with pumping or injection wells in confined isotropic aquifers with uniform regional flow is proposed and tested against steady-state and transient-state numerical simulations on MODFLOW-MODPATH. The solution is based on the complex potential theory and can be used for large numbers of arbitrarily positioned wells operated with different rates. The solution can be used to follow the movement of water particles in space (within pores or within the equivalent continuous media) and in time with two tracking modes: forward (from origin to target) and backward (from target to origin). The proposed solution is a useful tool that can be used for establishing groundwater resources management practices like designing groundwater remediation solutions, delineating capture zones, defining safeguard perimeters and mapping groundwater vulnerability. Moreover, the paper gives a comparative numerical study of flow fields near pumping wells, showing that, in terms of their shape and position, delineating capture zones using either steady-state or transient-state simulations would lead to practically similar results for long pumping periods. It is also shown that in such cases, the main differences between steady-state and transient-state simulation are present in the computed water particles' transport time.

Keywords Groundwater flow · Semi-analytical solutions · Pumping wells · Capture zone · Groundwater management

Introduction

Groundwater flow-fields analysis constitutes an important tool that is widely used in several hydrogeological problems—for

example, in flow fields generated by pumping wells, mapping streamlines can be useful for delineating capture zones (Christ and Goltz 2002), defining safeguard perimeters (Asadi-Aghbolaghi et al. 2011; Ataie-Ashtiani et al. 2012) and designing optimal pump-and-treat groundwater remediation solutions (Di Lena et al. 2013). From a groundwater flow perspective, the limit of the capture zone was considered by Shan (1999) as the line (or more exactly the streamline) that separates the water flowing down gradient from the water flowing towards a pumping well. While from a groundwater remediation point of view, the capture zone can be defined as the area of an aquifer out of which all the contaminated water will be removed by one or multiple well(s) within a certain amount of time (Grubb 1993). Optimizing this last definition, by selecting the proper locations, configuration and number of pumping wells to capture a plume of contaminated water (Fetter 1993) is the challenge facing the widely implemented pump-and-treat remediation strategy (Cohen et al. 1997).

Several research projects have tackled the capture-zone-delineation problem using mainly analytical or semi-analytical methods (Bear and Jacobs 1965; Christ and Goltz 2004) or using numerical approaches (Ahlfeld and Sawyer 1990; Cole and Silliman 2000). Due to its simplicity and its

Electronic supplementary material The online version of this article (<https://doi.org/10.1007/s10040-018-1869-0>) contains supplementary material, which is available to authorized users.

✉ Mohamed Amine Boukhemacha
boukhemacha-amine@hotmail.com

Ioan Bica
ioan.bica@utcb.ro

Ghiocel Groza
grozag@utcb.ro

¹ Department of Hydraulics and Environment Protection, Technical University of Civil Engineering Bucharest, Bd. Lacul Tei No. 122–124, 020396, sector 2, Bucharest, Romania

² Department of Hydraulics, National Polytechnic School, 10 Avenue Hassen Badi BP 182 El-Harrach, 16200 Algiers, Algeria

³ Department of Mathematics and Computer Science, Technical University of Civil Engineering Bucharest, Bd. Lacul Tei No. 122–124, 020396, sector 2, Bucharest, Romania

high adaptability, the complex potential theory has gained popularity amongst the analytical and semi-analytical approaches. This theory has been used to study different features describing groundwater flow fields: streamlines (Kompani-Zare et al. 2005), stagnation points (Lu et al. 2009), and capture zones (Christ and Goltz 2004). Such features were analyzed under different boundary conditions ranging from one or multiple pumping (Christ and Goltz 2002) or injection (Christ et al. 1999) wells, fully (Christ and Goltz 2002) or partially penetrating wells (Faybishenko et al. 1995), vertical (Grubb 1993) or horizontal (Kompani-Zare et al. 2005) wells, proximity to a stream (Asadi-Aghbolaghi et al. 2011), to areal recharge rates (Lu et al. 2009). The theory was applied on confined (Grubb 1993) and unconfined aquifers (e.g. Grubb 1993) under steady (Faybishenko et al. 1995; Grubb 1993) or unsteady flow regimes (Bear and Jacobs 1965; Yang et al. 1995) using simplifying assumptions on the aquifer's material (homogeneous and isotropic) and geometry (constant thickness).

With the aim of developing an efficient and flexible tool that can be used to describe groundwater flow fields associated with pumping or injection wells and to track the movement of water particles in space and time within such fields, a new semi-analytical solution is presented in this paper. The solution is derived by numerically solving a system of differential equations obtained from the complex potential theory. The predication capabilities of the proposed solution are demonstrated through a comparative study against steady-state and transient-state groundwater flow simulations and by computing safeguard perimeters. At this stage, the focus was not on the uncertainty of the input parameters used in the solution nor on the effects of the spatial variability of these parameters.

Background: complex flow theory for uniform regional flow and a pumping well

The flow regime resulting from pumping groundwater, with a flow rate Q , using a fully penetrating well tapping a homogeneous isotropic confined sedimentary aquifer with a constant thickness presenting a uniform regional flow with a Darcy velocity U , can be described mathematically using the complex flow potential theory as follows (e.g. Milne-Thompson 1968):

$$w = -U \cdot z - \frac{Q}{2\pi B} \ln(z - z_1), \text{ with } \begin{cases} z = x + iy \\ z_1 = x_1 + iy_1 \\ i^2 = -1 \end{cases} \quad (1)$$

where, w is the complex potential function of the resulting flow, U [L/T] is the Darcy flow velocity of the regional uniform flow parallel to the x -axis in the negative direction, Q [L³/T] is the discharge rate from the well, z is a complex variable describing the location of a point with coordinates (x, y) within a two-

dimensional (2D) space, z_1 is a complex variable describing the location of the pumping well with coordinates (x_1, y_1) , and B [L] is the thickness of the aquifer.

The expression of the complex potential given in Eq. (1) can also be used in the case of an injection well superimposed with a regional uniform flow by assigning a negative value for Q .

$$\begin{cases} w = \varphi + i\psi \\ \ln(z - z_1) = 0.5 \ln \left[(x - x_1)^2 + (y - y_1)^2 \right] + i \tan^{-1} \left(\frac{y - y_1}{x - x_1} \right) \end{cases} \quad (2)$$

Noting that the real part of the complex potential represents the velocity potential function φ while the imaginary part is stream function ψ , in addition to the expression of the logarithm of a complex number in terms of its modulus and argument (see Eq. 2), it is possible to write the velocity potential and stream functions as given in Eq. (3).

$$\begin{cases} \varphi = -U \cdot x - \frac{Q}{4\pi B} \ln \left[(x - x_1)^2 + (y - y_1)^2 \right] + C \\ \psi = -U \cdot y - \frac{Q}{2\pi B} \tan^{-1} \left(\frac{y - y_1}{x - x_1} \right) \end{cases} \quad (3)$$

where C is a constant. Additionally, the complex potential theory can be used to determine position (given by z_{SP} in complex form or by the coordinates (x_{SP}, y_{SP}) in the 2D space) of the stagnation point where the flow velocity is null (Milne-Thompson 1968) using Eq. (4).

$$\frac{dw}{dz} = 0 \Rightarrow z_{SP} = z_1 - \frac{Q}{2\pi B \cdot U}, \text{ or } \begin{cases} x_{SP} = x_1 - \frac{Q}{2\pi B \cdot U} \\ y_{SP} = y_1 \end{cases} \quad (4)$$

Furthermore, the theory can provide the mathematical expression of the capture zone of a well defined as the streamlines passing through the stagnation point (e.g. Milne-Thompson 1968). Note that the aforementioned development of the complex potential theory describes the flow regime in steady-state conditions and does not take account of the transient-state of the initial stages taking place immediately after the beginning of the pumping.

New semi-analytical solution

Let a hydrogeological system with groundwater flow conditions similar to those assumed in the previous section (a uniform regional flow and a pumping well) be considered. Given that the two components, the effective groundwater flow velocity vector along the x and y axes, can be written as:

$$\begin{cases} v_x = \frac{dx}{dt} = \frac{1}{n_e} \frac{\partial \varphi}{\partial x} \\ v_y = \frac{dy}{dt} = \frac{1}{n_e} \frac{\partial \varphi}{\partial y} \end{cases} \quad (5)$$

and using the expression of the velocity potential function (given in Eq. 3), it is possible to write the following autonomous system of differential equations:

$$\begin{cases} \frac{dx}{dt} = \frac{1}{n_e} \left[-U - \frac{Q}{2\pi B} \frac{x-x_1}{(x-x_1)^2 + (y-y_1)^2} \right] \\ \frac{dy}{dt} = \frac{1}{n_e} \left[-\frac{Q}{2\pi B} \frac{y-y_1}{(x-x_1)^2 + (y-y_1)^2} \right] \end{cases} \quad (6)$$

where v_x and v_y are the x -component and the y -component of the effective groundwater flow velocity respectively, n_e is effective porosity of the aquifer.

The obtained system of differential equations provides a mathematical formulation of the field of effective groundwater flow velocity under the previously considered conditions. Solving this system, in terms of $x(t)$ and $y(t)$, will describe the motion of water particles at different moments in time. To do so, a semi-analytical solution obtained using the Runge-Kutta method—see the electronic supplementary material (ESM) for more details—satisfying the initial conditions $x(t=0) = x_0$ and $y(t=0) = y_0$ is provided:

$$\begin{cases} x(t + \Delta t) = x(t) + \frac{\Delta t}{6} (A_{1,1} + 2A_{2,1} + 2A_{3,1} + A_{4,1}) \\ y(t + \Delta t) = y(t) + \frac{\Delta t}{6} (A_{1,2} + 2A_{2,2} + 2A_{3,2} + A_{4,2}) \end{cases} \quad (7)$$

with

$$\begin{cases} A_{1,k} = G_k[x(t), y(t)] \\ A_{2,k} = G_k \left[x(t) + \frac{\Delta t}{2}, y(t) + \frac{\Delta t}{2} A_{1,k} \right] \\ A_{3,k} = G_k \left[x(t) + \frac{\Delta t}{2}, y(t) + \frac{\Delta t}{2} A_{2,k} \right] \\ A_{4,k} = G_k [x(t) + \Delta t, y(t) + \Delta t A_{3,k}] \end{cases}, \quad k = 1, 2 \quad (8)$$

and

$$\begin{cases} G_1(x, y) = \frac{1}{n_e} \left[-U - \frac{Q}{2\pi B} \frac{(x-x_1)}{(x-x_1)^2 + (y-y_1)^2} \right] \\ G_2(x, y) = \frac{1}{n_e} \left[-\frac{Q}{2\pi B} \frac{(y-y_1)}{(x-x_1)^2 + (y-y_1)^2} \right] \end{cases} \quad (9)$$

where t is the time coordinate, and Δt is the time step used in the numerical solution.

Note that the proposed semi-analytic solution (given in Eq. 7) was derived using the effective groundwater flow velocity and can be adapted for Darcy flow velocity by replacing the effective porosity by 1. Furthermore, under its present form, the solution can be used to track the movement of a fluid particle within the pores of the aquifer materials from a given point of origin (whose coordinates constitute the initial conditions) to a target and thus it will be called a forward solution with a $\Delta t > 0$. A backward solution that can be used to track

the movement of a water particle from a target point to its origin can be easily obtained by using a negative time step ($\Delta t < 0$) and by taking as initial conditions the coordinates of the target point.

On the other hand, the developed solution with all its adaptations (i.e. forward and backward tracking, effective and Darcy velocity) can be extended for the case of hydrogeological systems with more than one pumping and/or injection wells. Such generalization to N wells is obtained by rewriting Eq. (9) as follows:

$$\begin{cases} G_1(x, y) = \frac{1}{n_e} \left[-U - \sum_{i=1}^N \frac{Q_i}{2\pi B} \frac{(x-x_i)}{(x-x_i)^2 + (y-y_i)^2} \right] \\ G_2(x, y) = \frac{1}{n_e} \left[-\sum_{i=1}^N \frac{Q_i}{2\pi B} \frac{(y-y_i)}{(x-x_i)^2 + (y-y_i)^2} \right] \end{cases} \quad (10)$$

where Q_i flow rate (taken to be positive for a pumping well and negative for an injection well) of the well i located at (x_i, y_i) .

Testing the new forward solution

In order to assess and demonstrate the prediction capabilities of the proposed solution (under its forward form), a comparative study against the US Geological Survey’s (USGS) MODPATH particle tracking code (Pollock 2016) is presented. The comparison is conducted in two ways: (1) in terms of the trajectory of water particles in space (i.e. the shape of the streamlines) which is an aspect that will consequently cover the shape and position of the capture zone, and (2) in terms of the time of their movement from one point to another (i.e. the shape of the isochrones).

The particle paths (which coincide with the flow streamlines under steady-state conditions) and isochrones computation on MODPATH were made using groundwater flow velocity fields generated from steady-state and transient-state groundwater flow models elaborated using the USGS MODFLOW (Harbaugh et al. 2000). A homogeneous isotropic confined aquifer with a constant thickness ($B = 10$ m) and an effective porosity $n_e = 0.3$ was considered. The regional uniform flow, parallel to the x -axis in the negative direction and with a $U = 0.01$ m/day, was obtained using specified head boundary conditions on the eastern and western boundaries of the spatial domain and no-flow boundary conditions on the northern and south boundaries (see Fig. 1). The spatial extent of the modeled aquifer was set to a 10×10 km square in order to reduce the impact of the specified head boundary conditions on the flow regime near the pumping well(s). The conducted numerical simulations consisted of introducing 1, 2 and 3 pumping well(s) in the central area of the uniform regional

flow under (1) steady-state and (2) transient-state groundwater flow conditions.

The so obtained groundwater flow velocity fields are then used to compute particle paths (representing also streamlines for steady-state) and isochrones (using MODPATH) for a set of water particles having as origin the line $x = 1,000$ m upstream of the well(s), as presented in (Fig. 1), spaced by 10 m (distance between two neighboring particles on the line of origin). The defined line of origin also represents the isochron $t = 0$. The choice of the location of this line of origin (and consequently the spatial extent of the particles tracking domain) was made in order to reduce the impact of the well(s) on the shape of the particles paths in the upstream area near the origin (i.e. a line that is close enough to the well but still produces particle paths that are initially virtually horizontal). The obtained features (streamlines/particle paths and isochrones) were compared to those computed using the proposed solution (forward tracking within the pores) under the same hydrogeological configurations using a time step $\Delta t = 2$ days.

The parameters of steady-state flow simulations

For a homogenous aquifer system under steady-state conditions under the used application's settings, the flow velocity field can be made independent of the hydraulic conductivity (K). This can be achieved by setting this parameter to any arbitrarily value (here taken as 1 m/day) and by using this value to compute the necessary specified head boundary conditions that would produce the desired uniform regional flow using Darcy' law (Eq. 11).

$$U = K \frac{(H_{US} - H_{DS})}{L} \quad (11)$$

where H_{US} [L] and H_{DS} [L] are the piezometric heads to be used on the eastern and western boundaries respectively, and L [L] is the length of the uniform regional flow (which is equal to the width of the modeled spatial domain).

The choice of the values of specified head boundary conditions was further conditioned by ensuring that the aquifer

will remain confined near the pumping wells. For the steady-state conditions, three simulations (SS1, SS2 and SS3) were developed using 1, 2 or 3 pumping wells. The parameters used for each simulation are given in Table 1.

The parameters and settings of transient-state flow simulations

Since the flow dynamic for a homogenous aquifer system under transient-state conditions will depend on the hydraulic conductivity (K) and the specific storage (S_s), parameters that are not accounted for in the complex potential theory, it was considered necessary to investigate the impact of the variability of these parameters on the response parameters (shape and position of particle paths and isochrones). To do so, a series of six transient simulations (TS1, TS2, ..., TS6) were generated using one pumping well by using different values of K (and consequently different values of H_{US} and H_{DS} computed using Eq. 11) and different values of S_s as summarized in Table 1. As for the settings of the numerical models, three stress periods (having lengths of 1, 999 and 79,000 days with 24, 20 and 30 numerical time steps respectively and producing a total length of the simulated period of 80,000 days) were used in MODFLOW for all transient-state simulations (such a choice was made to capture the rapid changes in the early stages of the pumping). The start of the pumping from the well was taken as $t = 0$ day and was used as origin of time when tracking the movement of particles. The initial conditions of each simulation were obtained from steady-state simulations under corresponding specified head boundary conditions with no pumping from the well.

Results and discussion

The streamlines/particle paths and isochrones computed using the proposed solution (under its forward tracking form of water particles within the aquifer materials' pores) for the considered simulations (with 1, 2 or 3 pumping wells) are

Fig. 1 Features and boundary conditions used in the numerical simulations in MODFLOW-MODPATH and in the proposed forward solution

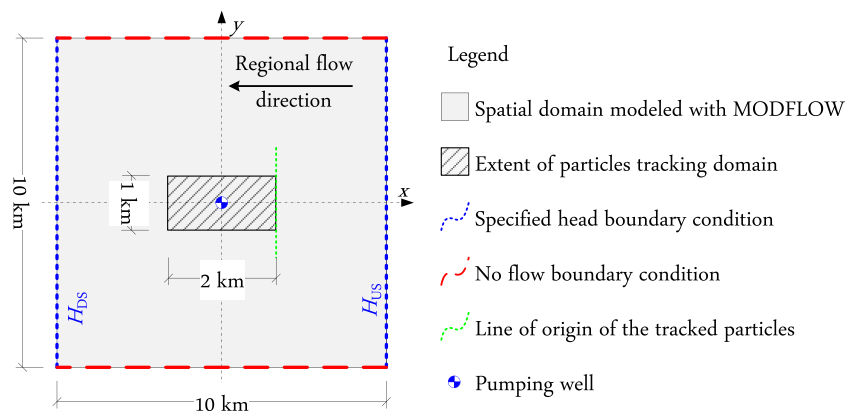


Table 1 Parameters used in the steady-state and transient-state groundwater flow simulation in MODFLOW

Flow regime	Simulation	Wells			Aquifer		
		Number	(x_i, y_i) [m]	Q_i [m ³ /day]	$H_{US} - H_{DS}$ [m]	K [m/day]	S_s [1/m]
Steady state	SS1	1	(0,0)	86.4	100	1	–
	SS2	2	(0,-50) (0,50)	43.2			
	SS3	3	(0,-100) (0,0) (0,100)	28.8			
Transient state	TS1	1	(0,0)	86.4	100	1	10^{-4}
	TS2				5	20	
	TS3				0.5	200	
	TS4				1	100	
	TS5						10^{-5}
	TS6						10^{-3}

compared to the MODFLOW-MODPATH modeling results from the developed nine simulations (summarized in Table 1). The comparison is conducted by pairs of simulations (in the form of new solutions against MODFLOW-MODPATH) having a matching number of wells, and results are presented and discussed for each flow regime.

New solution against steady-state simulations

For each one of the considered three simulations (in terms of the number of wells), the streamlines/particle paths and isochrones computed using the new solution are mapped against those obtained from MODFLOW-MODPATH simulations (see Fig. 2). Furthermore, in order to produce a more visible and quantifiable assessment of the difference between the results of the two used methods, the relative difference between the time of transport (RDTT) is computed as follows:

$$\text{RDTT}[\%] = \frac{t_{\text{NS}} - t_{\text{MP}}}{t_{\text{MP}}} \times 100 \quad (12)$$

where t_{NS} [T] and t_{MP} [T] is the transport time of a water particle from its origin (i.e. the line of origin) to a different position in its streamline computed using the new solution and MODFLOW-MODPATH simulations, respectively.

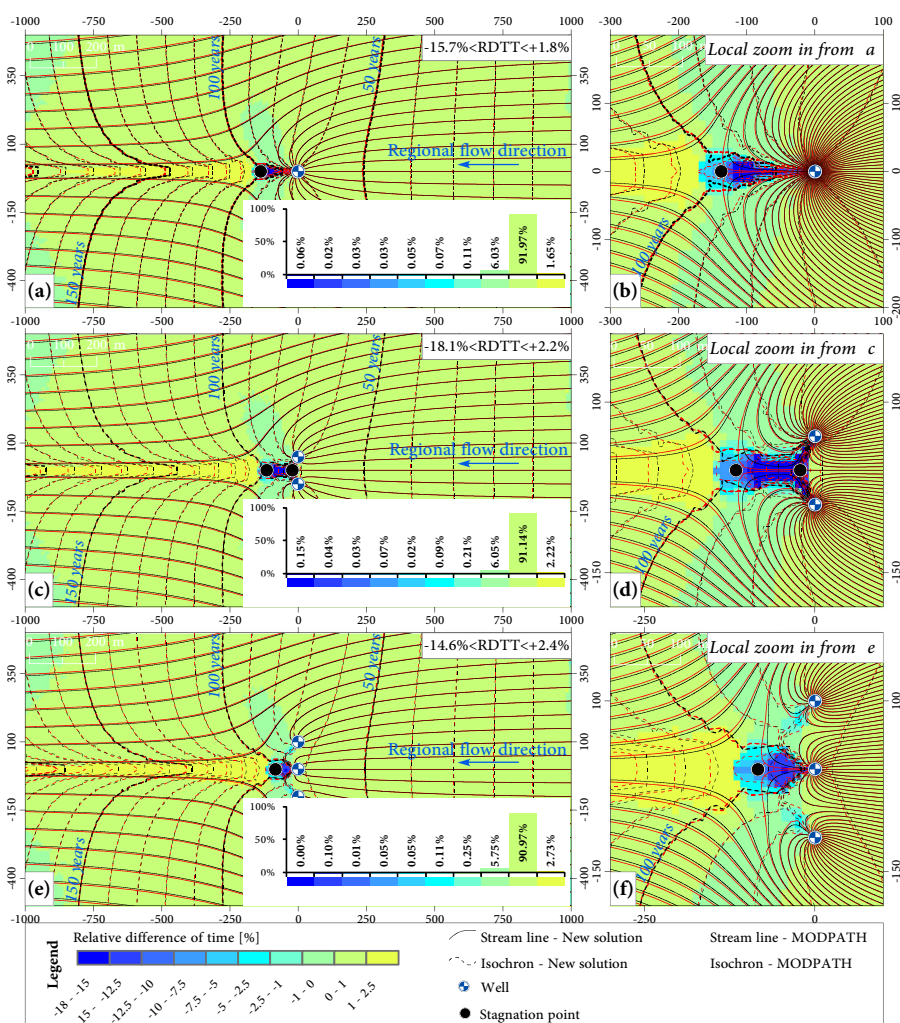
It can be easily observed on (Fig. 2) that in terms of shape and position, the streamlines obtained from the two methods are very close one from the other. These are practically overlapped in the region located upstream of the wells line (i.e. the line $x = 0$) and tend to be slightly separated the closer they get to the stagnation point or to the NW and SW corners of the mapped spatial domain. In statistical terms, the streamlines of all three simulations reflects very high values of Pearson correlation coefficients ($R^2 = 0.99$) for both x (computed using x coordinates of points on the compared streamlines sampled on

the basis of equal values of y) and y (computed using y coordinates of points on the compared streamlines sampled on the basis of equal values of x) coordinates. For the particular case of two wells (simulation SS2), an additional difference can be observed for the streamline(s) corresponding to the water particle generated at point (1000,0); MODFLOW-MODPATH streamlines do not account for the presence of the left-side stagnation point and go through it to reach either one of the two wells, whereas the streamline computed with the proposed solution do not continue beyond the stagnation point (Fig. 2c,b).

As for the differences between the shape and location of the isochrones, similar trends to those observed for the streamlines can be noticed. The differences in the area between the stagnation point and the well(s) is however more visible. In terms of magnitude, on the basis of the computed RDTT parameter, the relative absolute difference between the isochrones is mostly less than 1% (i.e. $-1\% < \text{RDTT} < 1\%$ on about 97% of the mapped spatial domain); the general trend indicates that the water particles' transport times computed with the new solutions are less than 1% higher than the values estimated with the steady state MODFLOW-MODPATH simulations. The largest differences in the computed transport time are observed in three areas:

1. *In the vicinity of the stagnation point with RDTT values up to -18% (covering an area less than 0.5% of the mapped spatial domain). These differences are mainly due to the fact that MODFLOW-MODPATH streamlines tends to get longer (as clearly shown in Fig. 2b,d,f) than those computed with the proposed forward solution the closer they get to the stagnation point (i.e. the water particles are following a longer path and thus higher transport time).*
2. *In the area downstream of the stagnation point (with RDTT values up to 2.5% over less than 3% of the area of the*

Fig. 2 Comparison between the new forward tracking solution and MODFLOW-MODPTAH simulations under steady-state flow in terms of streamlines/particle paths and isochrones for a regional uniform flow with: **a–b** one well, **c–d** two wells, **e–f** three wells (histograms: spatial coverage of each class of relative difference between the time of transport (RDTT) values expressed in %, reported to the total area of the mapped spatial domain)



mapped spatial domain). As for the previous area, the observed differences are principally associated to the length of the computed streamlines (the streamlines obtained using MODFLOW-MODPATH simulations are shorter than those computed with the proposed forward solution).

3. *Some fluctuation in the RDTT values can also be observed near the line of origin of particles, with RDTT values up to -2.5% over less than 1% of the area of the mapped spatial domain.* Note that these values do not necessarily reflect important differences in the length of streamlines nor large differences between the methods; absolute differences near the origin line where the transport time are small.

Even though, for the presented test, the largest differences between the proposed solution and MODPATH-MODFLOW results are obtained in the region close to the pumping well(s) (downstream the well(s) toward the stagnation point(s)), it must be noted that:

- The differences in the RDTT are in terms of cumulated transport time from the line of origin and do not

necessarily reflect low prediction capabilities of the proposed method in this area. However, in order to avoid propagating possible differences when analyzing flow dynamics near a well (e.g. well head protection area), it is recommended to use the backward solution (this reduces the cumulated differences in transport time) or the forward solution over shorter transport distances.

- Another aspect to keep in mind is that MODPATH does not account for stagnation points (as shown in Fig. 2d), which is believed to be the main cause of these differences, thus the differences do not necessarily indicate that the new solution is deviating for the exact solution.

New solution against transient-state simulations

For each one of the considered transient-state simulations (in terms of K and S_s), the particle paths and isochrones obtained from the five MODFLOW-MODPATH simulations are mapped against those computed using the new solution (see

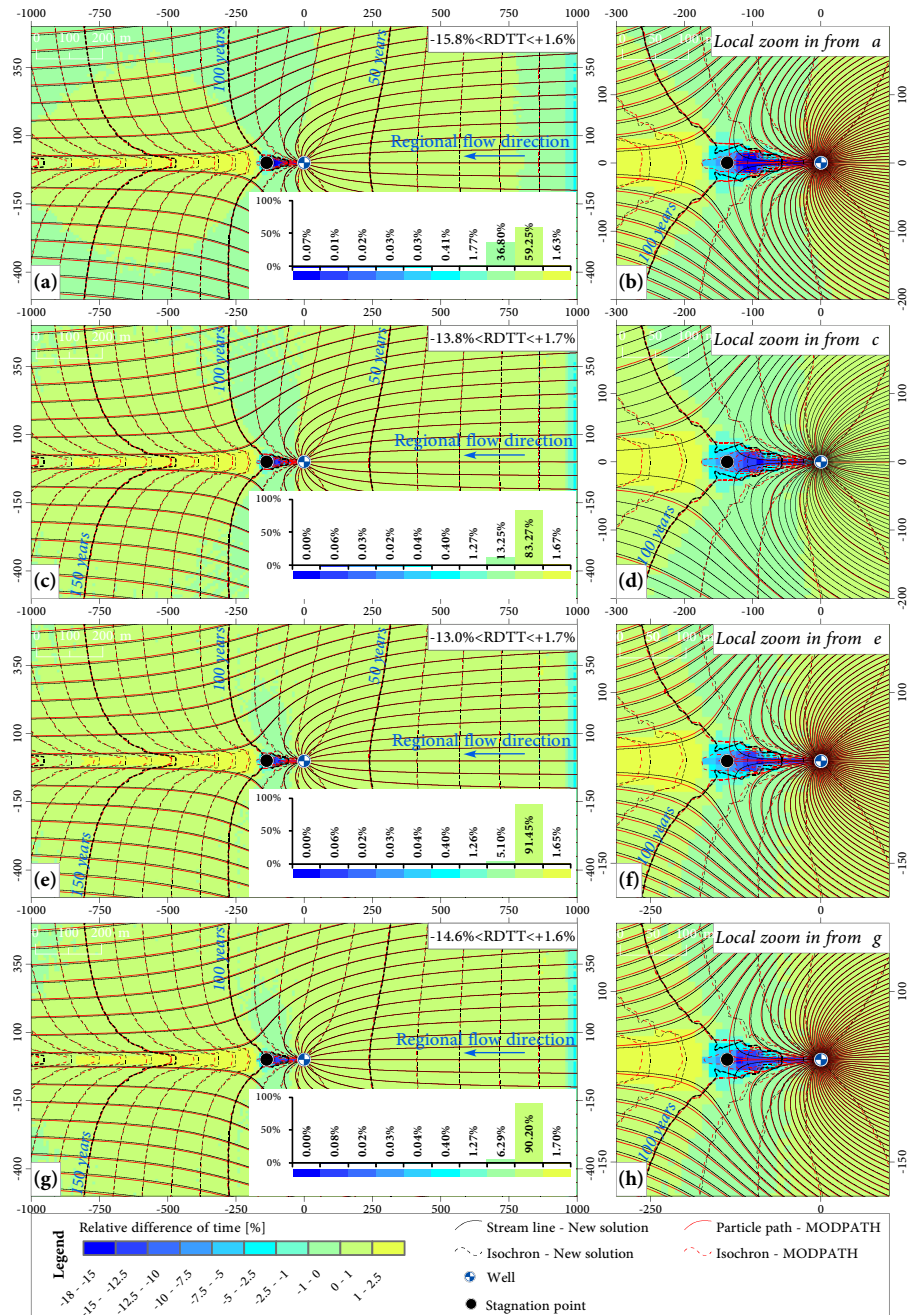
Figs. 3 and 4). The results are presented for each parameter separately.

Impact of the hydraulic conductivity (K)

Even using transient-state groundwater flow simulations with different values of K , the differences between the shapes and positions of the particle paths computed with the two methods are still barely noticeable and present similar patterns (see Fig. 3) as those obtained when comparing the new solution to steady-state simulations. The coefficient of correlations are still at the

0.99 level. As for the differences between the shapes and locations of the isochrones, similar trends are obtained. The relative absolute difference between the isochrones is still frequently less than 1% (i.e. $-1\% < RDIT < 1\%$ on 96% of the mapped spatial domain). However, the general trend seems to shift from RDDT values mostly within the interval -1 to 1% for lower K value to values mostly between 0 and 1% for the higher K value (i.e. new solution results are higher than the simulation). The largest differences in the computed transport time are always observed in the area of the stagnation point with RDIT values up to -15.8% and in the area downstream of the stagnation point (with RDIT

Fig. 3 Comparison between the new forward tracking solution and MODFLOW-MODPTAH simulations under transient-state flow in terms of particle paths and isochrones for a regional uniform flow with one well: **a–b** $K = 1$ m/day, **c–d** $K = 20$ m/day, **e–f** $K = 100$ m/day and **g–h** $K = 200$ m/day (histograms: spatial coverage of each class of RDIT values expressed in %, reported to the total area of the mapped spatial domain)



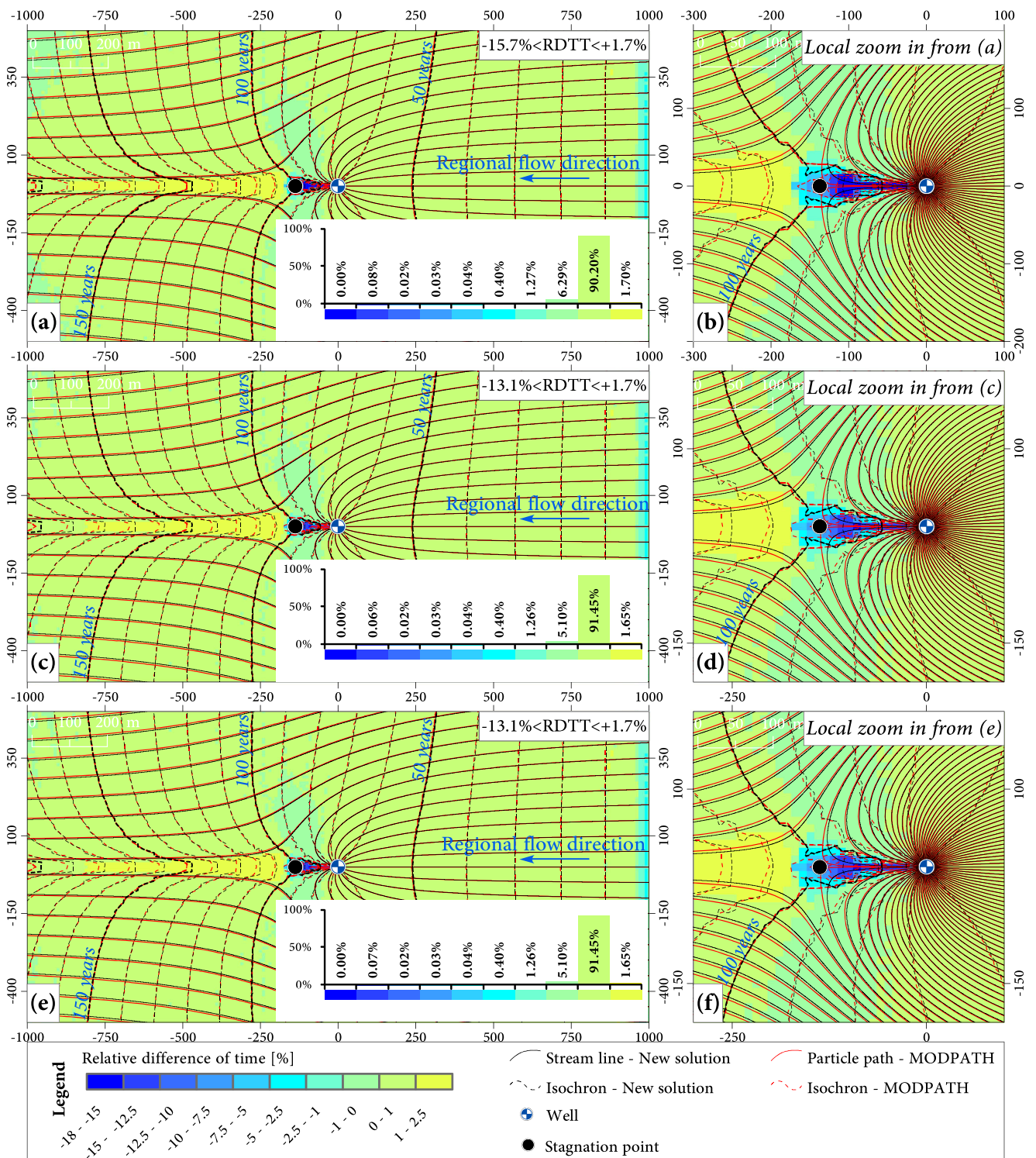


Fig. 4 Comparison between the new forward tracking solution and MODFLOW-MODPTAH simulations under transient-state flow in terms of particle paths and isochrones for a regional uniform flow with one well:

a–b $S_s = 10^{-5} \text{ m}^{-1}$, **c–d** $S_s = 10^{-4} \text{ m}^{-1}$ and **e–f** $S_s = 10^{-3} \text{ m}^{-1}$ (histograms: spatial coverage of each class of RDTT values expressed in %, reported to the total area of the mapped spatial domain)

values up to 2.5% over an area of about 2% of the mapped spatial domain). The fluctuations in the RDTT values near the line of origin of particles are more visible than those observed when comparing the new solution with steady-state solutions.

In all three previously identified areas, the differences in the RDTT values can be explained by the variation of the particle paths lengths (with similar trends as before). However, in contrast to the steady-state simulations, the

particle paths computed by transient-state MODFLOW-MODPATH simulations tend to get shorter the higher K gets (aspect leading to lower transport time). Moreover, the increased RDTT fluctuations' contrast (in comparison with steady-state simulations) near the origin line reflects the differences in the flow conditions at early stages of the flow between steady-state and transient-state MODFLOW simulations. In steady state the impact of the pumping well is felt from the start in the area of interest (near the line of origin); while in transient-state this effect is delayed.

Impact of the specific storage (S_s)

In the same manner, the use of transient-state groundwater flow simulations with different values of S_s does not appear to have a visible impact of the shape and the position of the particle paths leading to the same observation as previously (see Fig. 4) and comparable values of the coefficient of correlation ($R^2 = 0.99$) are obtained. The relative absolute difference between the isochrones is still frequently less than 1% (i.e. $-1\% < \text{RDTT} < 1\%$ on 96% of the mapped spatial domain). Similarly, the highest differences between the computed transport times are always observed in the area of the stagnation point (with RDTT values up to -15.7%) in the area downstream of the stagnation point (with RDTT values up to 2.5% over an area of about 2% of the mapped spatial domain) and in the vicinity of the particles' line of origin. The fluctuations in the RDTT values near this line are more visible than those observed in steady-state simulations.

Likewise, the differences in the RDTT values can be associated with variation of the particle paths' lengths. Likewise, the more visible RDTT fluctuations (in comparison with steady-state simulations) near the line of origin are due to the discrepancy in the flow conditions at early stages of the flow between steady-state and transient-state MODFLOW simulations.

Application of the new backward solution

Backward tracking a water particle for a given target to its source can be used, in a more efficient and easier way (compared to a forward tracking), to identify possible contamination sources as well as in defining safeguard perimeters. This last application is of great importance when establishing groundwater resources management practices. As a

demonstrative application, the proposed backward solution is used to define safeguard perimeters for a groundwater abstraction system. In order to further exemplify the flexibility of the new solution, in terms of well location and discharge rate, a pumping system composed of five fully penetrating wells arbitrary distributed in space and exploited with different discharge rates is considered (see Table 2). As before, a confined homogeneous and isotropic aquifer having a constant thickness ($B = 10$ m) with a similar uniform regional flow (parallel to the x -axis in the negative direction with a Darcy flow velocity $U = 0.01$ m/day) and an effective porosity $n_e = 0.3$ is used.

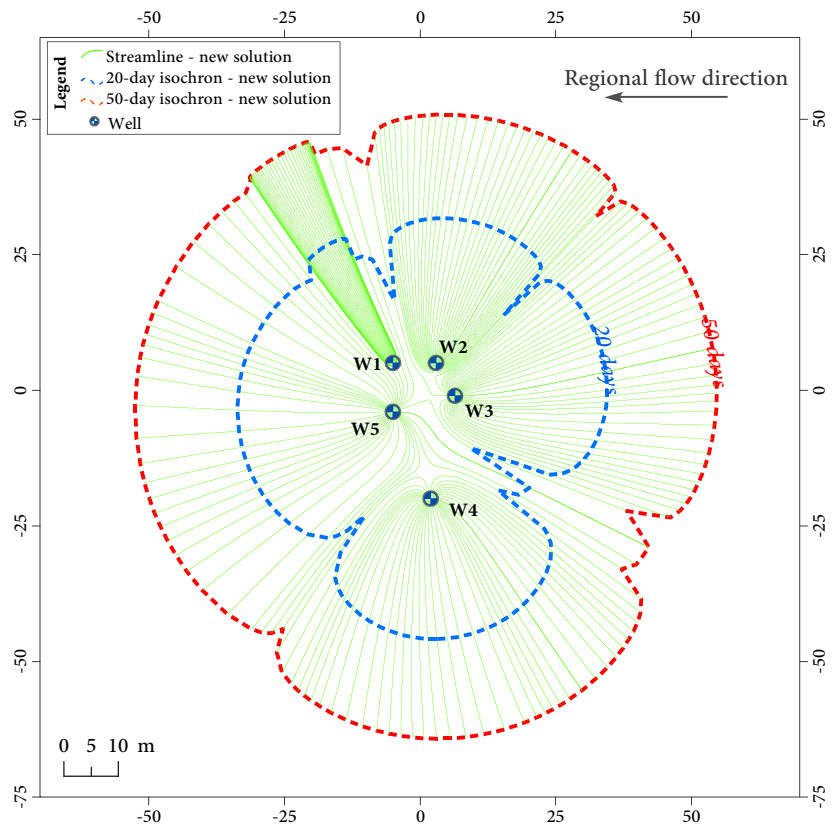
In agreement to the specification of the Romanian legislation (i.e. according to the Romanian-Water-Law-310/2004 and the Government Resolution HG-930/2005), two safeguard perimeters are defined: (1) the first one is called the "severe regime protection perimeter" and is delineated by the 20-day isochron and (2) the second, called the "restricted regime protection perimeter" is defined by the 50-day isochron. To define these perimeters, several streamlines (20 and 50 days long) and matching isochrones are computed with the backward solution using a negative time step of $\Delta t = -0.025$ day for sets of 37 particles per well distributed uniformly on the perimeter of each well (assumed to have a radius of 0.5 m). The location of each particle was used as the initial condition to compute its associated streamline/path. A small time-step value was necessary in this case, because the movement of water particles near a pumping well (in the near field) is very fast compared to the regional flow (which is predominantly in the far field). The obtained results are mapped in Fig. 5.

In terms of practical applications, even under its simplifying assumptions (homogeneous aquifer with a constant thickness and a uniform regional flow), the proposed solution falls within the recommendations of the US Environmental Protection Agency (EPA 1987) regarding the design of well-head protection areas. Jacobson et al. (2002) also reported that the use of similar simple approaches was found to be useful by many small municipalities considering the elevated cost linked to collecting large data sets from field investigations necessary to build detailed numerical models that would account for the spatial heterogeneity of the aquifer parameters and geometry. Similar practices are actually in agreement with the Romanian legislation (Government Resolution HG-930/2005) when dealing with abstractions with small discharge rates (less than 2 L/s).

Table 2 Characteristics of the groundwater abstraction system

Characteristic	Well				
	W1	W2	W3	W4	W5
Location (x,y) [m]	(-5.0,5.0)	(3.0,5.0)	(6.5,-1.0)	(2.0,-20.0)	(-5.0,-4.0)
Discharge rate [m ³ /day]	20	80	120	135	200

Fig. 5 Mapped 20 and 50-day safeguard perimeters obtained using the proposed backward solution



Summary and conclusions

The study of groundwater flow fields is a useful tool for establishing groundwater resources management practices. Designing groundwater remediation solutions, delineating capture zones and defining safeguard perimeters are amongst the most common applications. In the present work, a new semi-analytical solution that can be used to describe groundwater flow fields associated with pumping or injection wells, and to track the movement of water particles in space and times within such fields, is proposed and tested against numerical steady-state and transient-state simulations. The solution is based on the complex potential theory. It can be used with any number of arbitrarily distributed abstraction and/or injection wells operated with different flow rates and presents several innovative capabilities allowing the user to follow the movement of particles, within pores or within the equivalent continuous media, not only in space but also in time with two tracking modes: forward (from origin to target) or backward (from target to origin). Computations using this new solution are faster and easier than other existing methods (it does not involve solving several non-linear equations). In addition to the presented applications (flow field computation, capture zone delineation, stagnation points identification and safeguard perimeters delineation), it is believed that the proposed solution's capabilities can be further exploited in groundwater

vulnerability concepts, particularly when speaking of groundwater source vulnerability.

On the basis of the conducted comparative study, it was found that, by tracking particles generated in the far field (upstream of the well), the shape and position of the capture zone obtained using transient-state numerical simulations do not present significant differences from those obtained from steady-state simulations. For long pumping periods, transient-state simulations would account for changes in the flow field (originating at the well and progressively propagating within the zone of influence of the well) that take place at early stages (at the beginning of pumping), whereas in steady-state simulations, such perturbations are taken as fully developed from the start. Consequently, the main differences in the computed flow fields were found to be in the transport time; moreover, for transient-state simulations, given that a particular uniform regional flow can be generated from different specific storage and hydraulic conductivity values, the conducted simulations showed that changes in these parameters would affect the transport time more than (relatively speaking) they would affect the shape and the position of the particle paths and that the impact of the S_s was higher than that associated with changes in K .

Under the adopted simplifying assumptions (homogeneous aquifer with a constant thickness and a uniform regional flow), the proposed solution with its different adaptations treats input parameters as deterministic variables (taken in practice as

mean values). However, uncertainty in these parameters can be accounted for by conducting computations with several values of each parameters (defined statistically or stochastically) and by keeping the worst-case scenario in design practices.

Acknowledgements Particular thanks are given to the two anonymous reviewers, the editor and the associate editor for their helpful comments.

References

- Ahlfeld DP, Sawyer CS (1990) Well location in capture zone design using simulation and optimization techniques. *Groundwater* 28(4):507–512. <https://doi.org/10.1111/j.1745-6584.1990.tb01705.x>
- Asadi-Aghbolaghi M, Rakhshandehroo GR, Kompani-Zare M (2011) Analytical solutions for the capture zone of a pumping well near a stream. *Hydrogeol J* 19:1161–1168. <https://doi.org/10.1007/s10040-011-0741-2>
- Ataie-Ashtiani B, Shafei B, Rashidian-Dezfouli H, Mohamadzadeh M (2012) Capture zone of a partially penetrating well with skin effects in confined aquifers. *Transp Porous Media* 91(2):437–457. <https://doi.org/10.1007/s11242-011-9853-3>
- Bear J, Jacobs M (1965) On the movement of water bodies injected into aquifers. *J Hydrol* 3:37–57. [https://doi.org/10.1016/0022-1694\(65\)90065-X](https://doi.org/10.1016/0022-1694(65)90065-X)
- Christ JA, Goltz MN, Huang J (1999) Development and application of an analytical model to aid design and implementation of in situ remediation technologies. *J Contam Hydrol* 37:295–317. [https://doi.org/10.1016/S0169-7722\(99\)00002-9](https://doi.org/10.1016/S0169-7722(99)00002-9)
- Christ JA, Goltz MN (2002) Hydraulic containment: analytical and semi-analytical models for capture zone curve delineation. *J Hydrol* 262(1–4):224–244. [https://doi.org/10.1016/S0022-1694\(02\)00026-4](https://doi.org/10.1016/S0022-1694(02)00026-4)
- Christ JA, Goltz MN (2004) Containment of groundwater contamination plumes: minimizing drawdown by aligning capture wells parallel to regional flow. *J Hydrol* 286(1):52–68. <https://doi.org/10.1016/j.jhydrol.2003.09.012>
- Cohen RM, Mercer J, Greenwald M, Beljin MS (1997) Design guidelines for conventional pump-and-treat systems, ground water issue. EPA/540/S-97/504, USEPA, Washington, DC
- Cole BE, Silliman SE (2000) Utility of simple models for capture zone delineation in heterogeneous unconfined aquifers. *Groundwater* 38(5):665–672. <https://doi.org/10.1111/j.1745-6584.2000.tb02702.x>
- Di Lena YC, Elmore AC, Conroy J (2013) Effectiveness of capture zones generated by intermittent pumping of a PV-powered pump-and-treat system without energy storage. *Remediation* 23(3):111–122. <https://doi.org/10.1002/rem.21360>
- EPA (1987) Guidelines for delineation of wellhead protection areas. US Environmental Protection Agency report 440/6-87-010, USEPA, Washington, DC
- Faybishenko BA, Javandel I, Witherspoon PA (1995) Hydrodynamics of the capture zone of a partially penetrating well in a confined aquifer. *Water Resour Res* 31(4):859–866. <https://doi.org/10.1029/94WR02707>
- Fetter CW (1993) Contaminant hydrogeology. Macmillan, New York
- Grubb S (1993) Analytical model for estimation of steady-state capture zones of pumping wells in confined and unconfined aquifers. *Groundwater* 31(1):27–32. <https://doi.org/10.1111/j.1745-6584.1993.tb00824.x>
- Harbaugh AW, Banta ER, Hill MC, McDonald MG (2000) MODFLOW-2000, the U.S. Geological Survey modular ground-water model: user guide to modularization concepts and the ground-water flow process. US Geol Surv Open-File Rep 00-92
- Jacobson E, Andricevic R, Morrice J (2002) Probabilistic capture zone delineation based on an analytic solution. *Groundwater* 40(1):85–95. <https://doi.org/10.1111/j.1745-6584.2002.tb02494.x>
- Kompani-Zare M, Hongbin Z, Nozar S (2005) Analytical study of capture zone of a horizontal well in a confined aquifer. *J Hydrol* 307(1–4):48–59. <https://doi.org/10.1016/j.jhydrol.2004.09.021>
- Lu C, Gong R, Luo J (2009) Analysis of stagnation points for a pumping well in recharge areas. *J Hydrol* 373:442–452. <https://doi.org/10.1016/j.jhydrol.2009.05.002>
- Milne-Thompson LM (1968) Theoretical hydrodynamics. Macmillan, New York
- Pollock DW (2016) User guide for MODPATH Version 7-A particle-tracking model for MODFLOW. US Geol Surv Open-File Rep 2016–1086. <https://doi.org/10.3133/ofr20161086>
- Shan C (1999) An analytical solution for the capture zone of two arbitrarily located wells. *J Hydrol* 222(1–4):123–128. [https://doi.org/10.1016/S0022-1694\(99\)00101-8](https://doi.org/10.1016/S0022-1694(99)00101-8)
- Yang YJ, Spencer RD, Gates TM (1995) Analytical solutions for determination of non-steady state and steady-state capture zones. *Groundw Monit Remediation* 15:101–106. <https://doi.org/10.1111/j.1745-6592.1995.tb00507.x>